Icarus 197 (2008) 164–168

Contents lists available at ScienceDirect

Icarus

www.elsevier.com/locate/icarus

# Formation of smooth terrains on Comet Tempel 1

Akiva Bar-Nun [a,*], Finnur Pálsson [b], Helgi Björnsson [b]

[a] *Department of Geophysics and Planetary Science, Tel Aviv University, Ramat Aviv, Tel Aviv 69978, Israel*
[b] *Institute of Earth Sciences, Science Institute, University of Iceland, Sturlugata 7, IS-101, Reykjavík, Iceland*

ARTICLE INFO

*Article history:*
Received 16 October 2007
Revised 27 April 2008
Available online 29 May 2008

*Keywords:*
Comet Tempel-1
Comets, nucleus
Comets
Ices
Ices, mechanical properties

ABSTRACT

We suggest that the regions of smooth terrain which were observed on Comet 9P/Tempel 1 by the Deep Impact spacecraft were formed by blowing ice grains in an outburst of gas from the comet interior. When gas is released from 10 to 20 m deep layers which were heated to 135 K, it is released quiescently onto the surface by individual conduits. If large amounts of gas are released, the drainage system cannot release them fast enough and wider interconnected channels are formed, leading to sudden outburst of gas. Instability triggering a sudden shift of flow is well known in subglacial drainage of water. The ballistic trajectory of the ice particles reach a distance of 3 km in the atmosphereless comet, whose gravity is 0.034 $cm\,s^{-1}$, if ejected at an angle of 45° at a speed of 95 $cm\,s^{-1}$. This speed is close to the speeds measured in laboratory experiments: 167, $140 \times \sin \boldsymbol{i}$ and 167 $cm\,s^{-1}$, for particles of 0.3, 1000 and 14–650 μm, respectively. Blowing of ice grains can overcome the 1650 m long horizontal section of smooth terrain i1 (Fig. 1), whereas simple flow of material downhill would stop close to the foot of the hill. The ice particles at the end of their trajectory have a horizontal velocity component and this low velocity ballistic sedimentation would lead to formation of lineaments on the smooth terrain, like in solid-particulate volcanic eruptions.



## 1. Introduction

This introduction follows closely the discussion in Thomas et al. (2007): Deep Impact images of the nucleus of Comet Tempel 1 reveal two and possibly three areas of remarkably smooth terrain. These surfaces are completely devoid of craters and must be smooth at scales of less than 5 m. Two of these show definite evidence of displacement by flow and the better imaged of the two (region i1 in Fig. 1) is an elongated flow-like tongue about 3 km long, 1 km wide, and at least 20 m high. Along the long axis of the flow (Fig. 14 of Thomas et al., 2007) there is initially a downhill slope at about 5° for 850 m, which levels off between 850 and 1650 m, and reverses to uphill (−3°) between 1650 and 2100 m, leveling off up to 2500 m. Yet, Thomas in a personal communication says that the calculation of the uphill slope is marginal. Therefore, we shall assume that after the 5 degrees downhill section of 850 m, the surface levels off and remains horizontal for the remaining 1650 m. The terminal end shows finger-like markings suggestive of spreading (Figs. 13, 15, ibid). The other extensive area of smooth terrain (region i2 in Fig. 1) appears to fill part of a large arcuate depression, which trends downslope for some 2 km (Fig. 14, ibid). The probable source of region i1 is illuminated by light scattered from the crater ejecta, and region i2 seems to originate in *j* (Fig. 8, ibid), where Sunshine et al. (2006) found exposed water ice.

It seems unavoidable to Thomas et al. that the smooth areas represent material which has been erupted or otherwise released onto the surface, and that the material involved was very fluid, fine textured and homogeneous. It consists of typical "comet material" by not being distinct photometrically (Li et al., 2007). Several attempts were made to explain the mechanism of formation of the smooth terrains. Basilevsky and Keller (2007) propose a sublimation-driven collapse of relatively steep slopes and avalanche-like distribution of the collapsed material within the gravitation potential lows. Belton et al. (2007) propose channeling of slowly moving ejecta flow by the local topography. Both mechanisms will be discussed below.

In what follows, we shall attempt to find a mechanism which could possibly form these smooth terrains and lineaments. First, some physical parameters regarding Comet Tempel 1, based on the findings of Deep Impact (A'Hearn et al., 2005; A'Hearn and Combi, 2007; Thomas et al., 2007; Richardson et al., 2007) and supported by our experimental results on large samples (20 cm diameter and 10 cm high) of gas-laden amorphous ice, which agree well with Deep Impact's findings (Bar-Nun and Laufer, 2003; Laufer et al., 2005; Bar-Nun et al., 2007). The parameters are labeled DI for Deep Impact and EXP for our experiments.

* Corresponding author.
*E-mail addresses:* akivab@post.tau.ac.il (A. Bar-Nun), fp@raunvis.hi.is (F. Pálsson), hb@raunvis.hi.is (H. Björnsson).

0019-1035/$ – see front matter 
doi:10.1016/j.icarus.2008.05.007

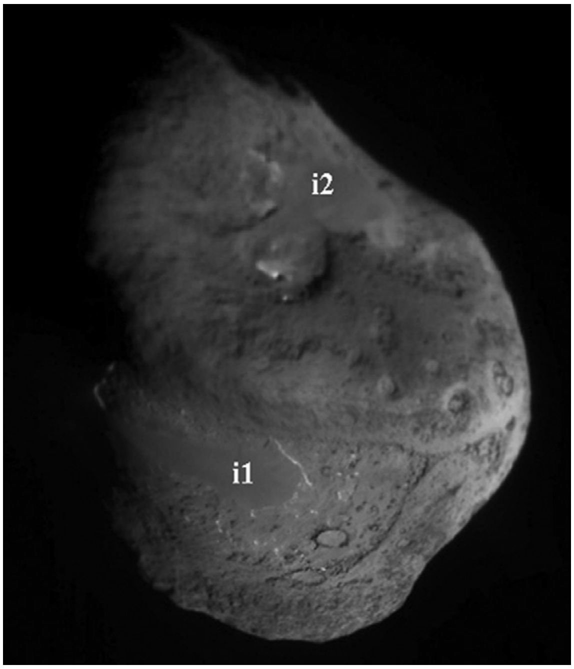


**Fig. 1.** Smooth terrains i1 and i2 on Comet Tempel 1 (NASA).

Size of region i1: 3 km × 1 km × 20 m—DI (Thomas et al., 2007)
$\alpha$, slope in i1 region:
downhill 5°, up to 850 m from origin—DI (ibid)
0° at 850–1650 m and 2100–2600 m
uphill (−3)° at 1650–2100 m
OR
horizontal between 850 and 2600 m

This is a major point to be considered when explaining the mechanism of formation of the smooth terrains. If a flow downhill is proposed, then a flow over a horizontal terrain 1650 m long has to be explained as well.

$\alpha$, slope in i2 region: 7° up to 300 m from origin—DI (ibid)
3° at 300–2100 m
Gravitational acceleration: $g = 0.034\ \mathrm{cm\,s^{-2}}$—DI (Richardson et al. 2007)
Density: $\rho = 0.4\ \mathrm{g\,cm^{-3}}$—DI (Richardson et al., 2007)
$\rho = 0.25$–$0.30\ \mathrm{g\,cm^{-3}}$—EXP

Tensile strength: 0.065 kPa—DI (A'Hearn et al., 2005)
0–12 kPa—DI (Holsapple and Housen in A'Hearn et al., 2005)
Effective strength: 1–10 kPa—DI (Richardson et al., 2007)
Tensile strength: 2–4 kPa—EXP
Surface temperature: $T = 272$–$336$ K—DI (Groussin et al., 2007).
Thermal inertia: $I < 50\ \mathrm{W\,K^{-1}\,m^{-2}\,s^{-1}}$—DI (Richardson et al. 2007)
$I < 100\ \mathrm{W\,K^{-1}\,m^{-2}\,s^{-1}}$—EXP

Comet material devoid of volatiles—down to 1 m from the surface (Sunshine et al., 2007). Unheated and unaltered comet material—at 10–20 m below surface (ibid).

Of special importance to our proposed mechanism is the close agreement in the ice parameters: density, tensile strength and thermal inertia, between our experimental ice sample and the properties of the upper layers of Comet Tempel 1, as found by Deep Impact. This means that we can use our experimental findings to study processes on Tempel 1.

## 2. The proposed mechanism of formation of smooth terrains

### 2.1. Creeping of ice downhill

We tried first to see whether creeping of polycrystalline ice can account for the smooth terrain, assuming that some viscous ice emerged from an opening and crept along the slope. From basic physics of glaciers (Paterson, 1994), the surface flow velocity due to deformation

$$U_D = \big(2A/(n+1)\big)h\tau^n, \tag{1}$$

where $n$ is a constant varying between 1.5 and 4.2, with a mean about 3, $h$ is the height of the ice layer and $A$ is a measure of the creep.

The relation between the shear strain rate $\varepsilon$ and the shear stress $\tau$ is of form

$$\varepsilon = A\tau^n. \tag{2}$$

Thus the flow of ice differs markedly from that of a viscous fluid, for which $n = 1$ and $1/A$ is the viscosity.

The shear stress is

$$\tau = \rho g h \times \sin\alpha, \tag{3}$$

where $\rho$, $g$, $h$ and $\alpha$ are density, acceleration due to gravity, the height of ice layer and the slope, respectively.

A varies with the temperature according to

$$A = A_0 \exp(-Q/RT), \tag{4}$$

where $Q$, the activation energy for creep or for volume self diffusion, is about 60 $\mathrm{kJ\,mol^{-1}}$. For hexagonal ice at 273 K $A = 6.8 \times 10^{-15}\ (\mathrm{kPa})^{-3}\,\mathrm{s^{-1}} = 2.15 \times 10^{-16}\ \mathrm{Pa^{-3}\,yr^{-1}}$ given: $\rho = 350\ \mathrm{kg\,m^{-3}}$, $g = 3 \times 10^{-4}\ \mathrm{m\,s^{-2}}$, $h = 20$ m and $\alpha = 5°$ for region i1: $\tau = 0.2$ Pa and the surface flow velocity $U_D = (2A/(n+1))h\tau^n = 2 \times 10^{-16}\ \mathrm{m\,yr^{-1}}$. This extremely small velocity due to deformation stems from the very low driving force due to gravity and will remain very small even if the values used in the calculation were somewhat different. It should be stressed that even if the flowing material had no viscosity at all, it would not have flown uphill at a slope of −3° for 400 m.

### 2.2. Sliding of ice downhill

In addition to creeping of ice which requires deformation of the ice, if some viscous ice emerges from an opening it can slide downhill. Glaciers slide when lubricated by liquid water or by wet sediments underneath the ice, while sliding on a very dry bed is hindered by the high friction (Clarke, 2005). Solid–solid friction, very low $g$ and the horizontal topography for 1650 m will resist the sliding, even if a large source of viscous ice exists uphill.

An alternative is the emergence from a source uphill of a large amount of powdery ice and its flow downhill and then over a horizontal terrain for 1650 m. We find this scenario very unlikely for two reasons: First, the very low gravitational acceleration cannot provide a driving force to push the ice powder over the long horizontal terrain. Rather, the ice powder will pile up close to the bottom of the hill. Second, as shown above, the ice properties measured in our experiments are similar to those of the upper layers of Comet Tempel 1. In all of our experiments we have never seen any free flow down a slope of our dust-like, fluffy, ice sample. A tensile strength of 1–10 kPa prevents such movement, let alone creeping on a horizontal plateau. Thus we cannot see how the mechanisms proposed by Basilevsky and Keller (2007) and by Belton et al. (2007) would operate. Moreover, in our experiments, when a large flux of gas emanates from deep layers, the overlying ice layer is shattered and a massive flow of ice grains is observed, rather than a slow stream of ice particles oozing from the openings.

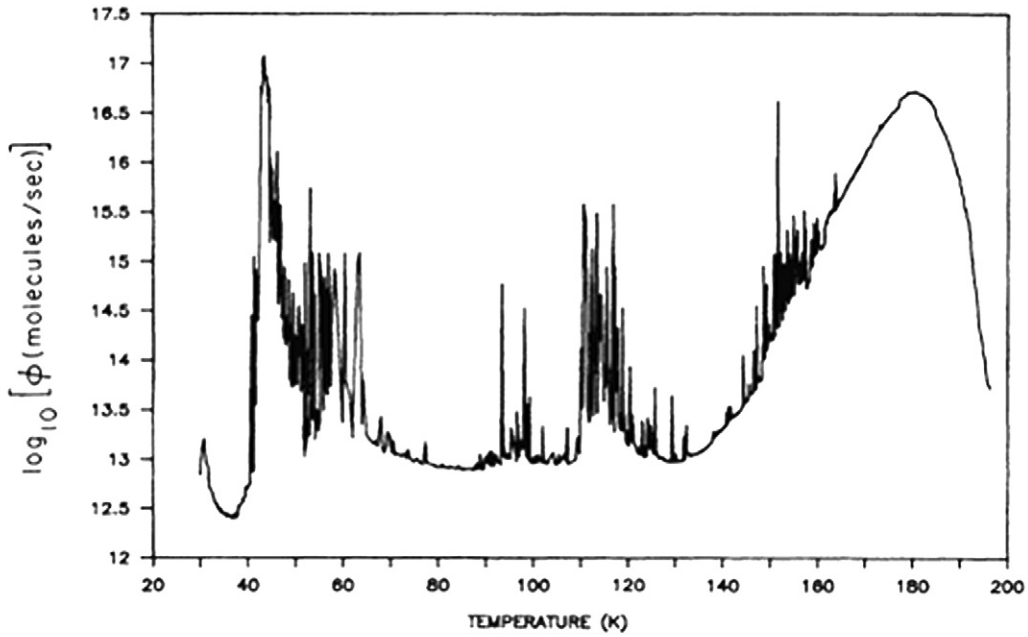


**Fig. 2.** Ice grain ejection from a thin ~100 μm gas-laden amorphous ice sample during various changes in the structure of the ice (from Laufer et al., 1987).

## 3. The outburst mechanism

Next, we tested the outburst mechanism, in which outbursts from a slanted opening carried ice grains to a distance of up to 3 km, to form the smooth terrains of i1 and i2. Grain ejection is observed experimentally whenever massive gas flow occurs from "cometary" ice or mineral–ice samples. We describe first the experiments from our laboratory at Tel-Aviv University and then those of KOSI at DLR in Köln.

### *3.1. Ejection of ice grains*

A thin, up to 100 μm layer of gas-laden amorphous ice was formed by flowing mixtures of water vapor + gas onto a cold plate at 20–50 K. The amorphous ice formed at these temperatures has many cavities in which gas is held through van der Waals forces until another ice layer forms above them, thus sealing the gas in the ice. Upon its warming up the amorphous ice anneals up to 120 K, transforms into the cubic structure at 135 K, into the hexagonal structure at ~160 K and, finally, sublimates completely at about 180 K. All these changes in the ice structure open some of the gas filled pores and let the gas escape. When gas pressure builds up in the ice, it shatters the overlying ice layers and the massive flow of gas carries with it the fragments (Fig. 2). Ice grains were observed by the mass spectrometer facing the ice sample (Bar-Nun et al., 1985; Laufer et al., 1987). On the average, each ice grain contains $10^9$–$10^{10}$ water molecules which, with a density of 0.3 $\mathrm{g\,cm^{-3}}$, has a radius of 0.3 μm. The average grain speed is $v \geqslant 167\ \mathrm{cm\,s^{-1}}$.

A large (20 cm diameter and 10 cm high) sample of gas-laden amorphous ice was prepared in the following way (Bar-Nun and Laufer, 2003): a mixture of water vapor with gas was flowed onto a cold plate at 80 K. When a 200 μm layer of gas-laden amorphous ice was formed, it was scraped from the plate by a 80 K knife and fell into the 80 K sample container. When an up to 10 cm thick sample, consisting of 200 μm ice grains and having a density of 0.25–0.3 $\mathrm{g\,cm^{-3}}$ was accumulated, it was warmed up from above by IR radiation from a hot dome, emitting 0.8–1.3 solar constants (1.37 kW). Gas evolution from the sample, when the heat wave moved inward, warming the gas-laden ice to 135 K, and water sublimating from the surface, were monitored by a mass spectrometer. Large changes in the ice, such as bulging due to gas pressure, shattering of the ice and ice grain ejection were followed by a video camera (Fig. 3). Ice grains of about 1 mm were seen to fly at an average speed of $v = 140 \times \sin \boldsymbol{i}\ \mathrm{cm\,s^{-1}}$, where $\boldsymbol{i}$ is the angle between the particles trajectory and a plane perpendicular to the ice sample's surface (Laufer et al., 2005; Pat-El, 2007, Ph.D. thesis). The gas jets which propelled the ice grains had a thermal velocity $6.7 \times 10^4\ \mathrm{cm\,s^{-1}}$, much larger than the particles speed.

In the KOSI (Komet Simulation Experiments) at DLR Köln (Grüen et al., 1993; Kölzer et al., 1995) a slurry of minerals with a trace of black carbon in water was sprayed into liquid nitrogen and mixed with solid $CO_2$ ice. When the 29 cm diameter and 13 cm high sample container was pumped on in the simulation chamber the liquid nitrogen evaporated, leaving in the container a porous sample (~0.5 $\mathrm{g\,cm^{-3}}$) of hexagonal ice particles with mineral dust, in which were dispersed solid $CO_2$ particles. The ice sample was tilted to 40° and irradiated by Xe arcs at a flux around 1 solar constant. A flux of water vapor and $CO_2$, initially at $1.5 \times 10^{18}\ \mathrm{cm^{-2}\,s^{-1}}$ was measured, which declined gradually to $5 \times 10^{17}\ \mathrm{cm^{-2}\,s^{-1}}$ after 500 min of irradiation and $4 \times 10^{17}\ \mathrm{cm^{-2}\,s^{-1}}$ after 590 min. The particle count rate followed the gas flux, being initially 60 $\mathrm{s^{-1}}$, falling to ~10 $\mathrm{s^{-1}}$ after 500 min and practically 0 after 590 min. Scanning electron microscope of the dust particles showed sizes of 14 μm for single mineral grains, up to 700 μm for agglomerates. Their densities ranged between 3 $\mathrm{g\,cm^{-3}}$ for a single grain, down to 0.2 $\mathrm{g\,cm^{-3}}$ for 700 μm agglomerates. Their size distribution suggests a power low $N_{(c)} = N_0 C^{-\nu}$, where $C$ is the cross section of the particle. $N_0$, the normalization factor was found to be between $5.1 \times 10^6$ and $0.68 \times 10^6\ \mathrm{s^{-1}}$ at 30–70 s and 150–450 s after the onset of irradiation, while $\nu$, the distribution index, ranged between 1.9 and 1.8, respectively. The trajectories and speeds of the particles were followed photographically. Their highest speed was 167 $\mathrm{cm\,s^{-1}}$, remaining similar even 475 min after the beginning of irradiation. This speed is similar to our findings of 167 and $140 \times \sin \boldsymbol{i}\ \mathrm{cm\,s^{-1}}$ for the speed of the ice particles. Their acceleration vectors, however, varied considerably both in direction and magnitude, ranging between 10 $\mathrm{cm\,s^{-2}}$ at the beginning and 0.17 $\mathrm{cm\,s^{-2}}$ after 475 min of irradiation.

In conclusion, regardless of the size, shape and density of the particles, their speeds were always around 150 $\mathrm{cm\,s^{-1}}$. This con-

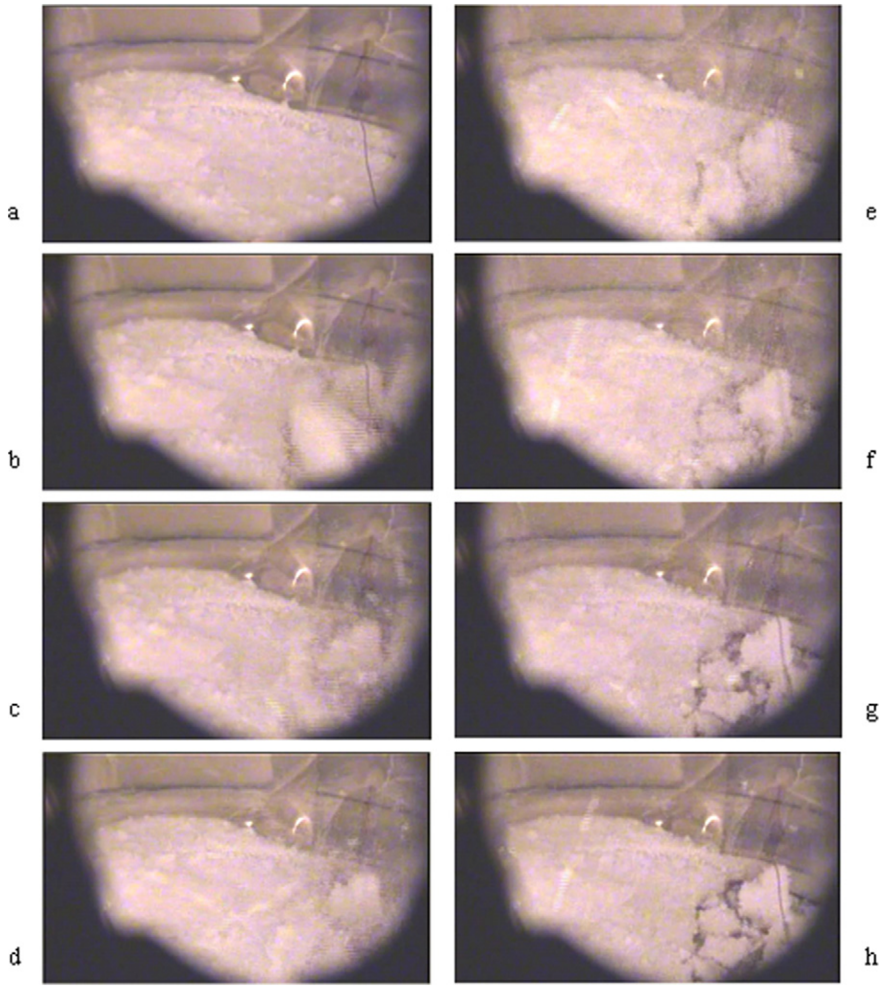

**Fig. 3.** Time sequence of swelling (b), breakage, and collapse in 1.5 cm thick ice samples. The magnitude of the collapse is best seen in (h). Note the ice grains seen in (d)–(f) and (h) (from Laufer et al., 2005). The grains are seen as faint streaks on the ice background.

stancy suggests that the size of the ice or ice–mineral particle which is broken from the matrix and propelled by the gas explosion, is similar to the size of the cavity in which the gas resides. Namely, in a fine grained ice sample, explosions of small cavities suffice to break and propel small particles, whereas in a coarse grained ice sample, explosion of large cavities break and propel large particles.

### *3.2. The outburst mechanism*

The particles which break from the ice matrix are propelled by momentum transfer from the gas which was released explosively. The drag coefficient in the KOSI experiments was calculated to be $5.4 \pm 2$, up to $10.3 \pm 3$.

Once out of the ice matrix, the particle follows a ballistic trajectory which, in the absence of an atmosphere, reaches a distance

$$R = v_0^2 \sin 2\theta / g, \tag{5}$$

where the acceleration due to gravity $g = 0.034\ \mathrm{cm\,s^{-2}}$, $v_0$ is the initial velocity and $\theta$ the angle between the surface and the particle's initial direction. Given $R = 3$ km, the length of the smooth region i1 and $\theta = 45°$, $v_0 = 95\ \mathrm{cm\,s^{-1}}$, as compared with $167\ \mathrm{cm\,s^{-1}}$ measured for 0.35 μm ice particles in thin ice samples, $140 \times \sin \boldsymbol{i}\ \mathrm{cm\,s^{-1}}$ measured for 200 μm ice particles in large ice samples and up to $167\ \mathrm{cm\,s^{-1}}$ for 10–650 μm dust–ice particles measured in the KOSI experiments. Changes in $\theta$, the angle of ejection will spread the ejecta along the entire 3 km length of the smooth region i1 on Tempel 1. The length ∼3 km vs width ∼1 km of the smooth region suggests that the emission of ice–dust particles is quite collimated. Namely, its source is below the surface. Sunshine et al. (2007) suggest that water ice exists already ∼1 m below the surface, while at a depth of 10–20 m the very low thermal conductivity results in unaltered ice. Namely, gas-rich amorphous water ice, from which gas is released upon warming up and propels ice particles on its way to the surface. A 10–20 m long channel will collimate the flow of ice particles. A ballistic trajectory will keep the ice particles in flight for $\tau = 2v_0 \sin\theta / g = 67$ min, whereas Sunshine et al. (2007) observed water ice particles up to 45 min. Thus the particles falling on the surface will consist of water ice. The rather sharp edge or scarp, 20 m high is not likely to result from this formation mechanism, which would prefer a gradual thinning of the deposit. Perhaps the observed scarp is a result of faster sublimation of the loosely packed pristine ice. It is worth mentioning that the entire smooth terrain, being pristine ice not yet covered by an insulating dust layer, would sublimate fast, until a dust layer is formed on it.

The lineaments of region i1, as seen in Figs. 8, 13 and 15 of Thomas et al. (2007), could arise from the impact of particles coming at an angle to the surface. Their horizontal velocity at the end of the trajectory will be their initial one which, for $v_0 = 1\ \mathrm{m\,s^{-1}}$ and $\theta = 45°$, is $v_0 \sin\theta = 0.7\ \mathrm{m\,s^{-1}}$. Their impact on the surface will result in low-velocity ballistic sedimentation and formation of lineaments, like in solid particulate volcanic eruptions. This movement should occur while the particles are still free to move. Once heated, they adhere to each other by the backflow of water vapor from the ice surface and form a crust (Laufer et al., 2005; Bar-Nun et al., 2007). This mechanism could explain the shape of region i1 but not that of i2. Here we have to assume two sources one at the bottom and one at the left hand corner (Fig. 1). The volume of ice + dust required for a layer 3 km × 1 km × 20 m is $6 \times 10^7$ m$^3$. Could this amount be ejected from near the comet surface and by which mechanism? When the 135 K front reaches into deeper layers in the comet nucleus, in the case of Tempel 1 to about 10–20 m, a large fraction of the trapped gas is released. We envision that the gas may typically be released from the ice on comets in a quiescent mode from a distributed gas drainage system. Dynamic percolation produces a distributed gas drainage system consisting of a network of variable widths. The quiescent release of gas from the ice (Bar-Nun and Laufer, 2003) is accompanied by grain ejection when the gas flow is large. Formation of even larger gas pockets *near the surface* results in the shattering of the overlying ice, massive gas release and formation of chaotic terrain (Laufer et al., 2005).

However, in comets, if the gas is released in deeper layers, it may act as a fluid where the drainage system cannot release it fast enough to the surface. We suggest that this may lead to the formation of a wider channel and a sudden outburst carrying with it ice particles to the surface, depositing them downstream according to their ballistic trajectories. Instability triggering a sudden shift of flow is well known in flow dynamics and we feel tempted to point out an analog shift from slow to fast flow in subglacial drainage of water (Kamb, 1987; Björnsson, 1998).

The driving force for this outburst is the penetration of the heat wave to deeper layers, which were not heated before to 135 K and still retain their trapped gases. We can therefore suggest that it could operate if favorable conditions prevail in the interior, at a periodicity of about 5.5 years, which is the current orbital period of Comet Tempel 1.

## 4. Conclusion

The smooth terrains observed on Comet Tempel 1 by the Deep Impact mission can be formed by a collimated flow of ice particles from a channel 10–20 m deep, driven by a massive flow of gas. The gas is released at 10–20 m below the surface when the heat wave reaches a layer of yet unaltered, gas-laden amorphous ice. The gas drainage system cannot release the gas fast enough and wider interconnected channels are formed, leading to a sudden release of gas, which carries with it the ice grains. The ballistic trajectories of the ice particles reach a distance of up to 3 km in the atmosphereless comet, whose gravity is 0.034 $\mathrm{cm\,s^{-2}}$, if ejected at 45° at a speed of 95 $\mathrm{cm\,s^{-1}}$. This speed is close to the speeds measured in laboratory experiments: 167, $140 \times \sin \boldsymbol{i}$ and 167 $\mathrm{cm\,s^{-1}}$, for particles of 0.3, 1000 and 14–650 μm, respectively, all under a massive flow of gas being released from the ice. Thus unlike a simple downhill flow of very loose ice, which cannot be pushed over 1650 m of horizontal terrain of region i1, the proposed mechanism overcomes this obstacle. Impacts by the particles at the end of their trajectories move the ice particles forward, in a process of low-velocity ballistic sedimentation, which produces the observed lineaments, like in solid particulate volcanic eruptions.

## Acknowledgments

We thank Michael Belton and James Richardson for many helpful suggestions.

## References

A'Hearn, M.F., Combi, M.R., 2007. Deep Impact at Comet Tempel 1. Icarus 187, 1–3.
A'Hearn, M.F., and 32 colleagues, 2005. Deep Impact: Excavating Comet Tempel 1. Science 310, 258–264.
Bar-Nun, A., Laufer, D., 2003. First experimental studies of large samples of gas-laden amorphous "cometary" ices. Icarus 161, 157–163.
Bar-Nun, A., Herman, G., Laufer, D., Rappaport, M.L., 1985. Trapping and release of gases by water ice and implications for icy bodies. Icarus 63, 317–332.
Bar-Nun, A., Pat-El, I., Laufer, D., 2007. Comparison between the findings of Deep Impact and our experimental results on large samples of gas-laden amorphous ice. Icarus 187, 321–325.
Basilevsky, A.T., Keller, H.U., 2007. Craters, smooth terrains, flows, and layering on the comet nuclei. Sol. Syst. Res. 41, 109–117.
Belton, M.J.S., and 14 colleagues, 2007. The internal structure of Jupiter family cometary nuclei from Deep Impact observations: The "talps" or "layered pile" model. Icarus 187, 332–344.
Björnsson, H., 1998. Hydrological characterization of the drainage system beneath a surging glacier. Nature 395, 771–774.
Clarke, G.K.C., 2005. Subglacial processes. Annu. Rev. Earth Planet. Sci. 33, 247–276.
Groussin, O., A'Hearn, M.F., Li, J.-Y., Thomas, P.C., Sunshine, J.M., Lisse, C.M., Meech, K.J., Farnham, T.L., Feaga, L.M., Delamere, W.A., 2007. Surface temperature of the nucleus of Comet 9P/Tempel 1. Icarus 187, 16–25.
Grüen, E., Gebhard, J., Bar-Nun, A., Benkhoff, J., Dueren, H., Eich, G., Hische, R., Huebner, W.F., Keller, H.U., Klees, G., 1993. Development of a dust mantle on the surface of an insolated ice–dust mixture—Results from the KOSI-9 experiment. J. Geophys. Res. 98, 15091–15104.
Kamb, B., 1987. Glacier surge mechanism based on linked cavity configuration of the basal water conduit system. J. Geophys. Res. 92, 9083–9100.
Kölzer, G., Grün, E., Kochan, H., Lämmerzahl, P., Thiel, K., 1995. Dust particle emission dynamics from insolated ice/dust mixtures: Results from KOSI 5 experiment. Planet. Space Sci. 43, 391–407.
Laufer, D., Kochavi, E., Bar-Nun, A., 1987. Structure and dynamics of amorphous water ice. Phys. Rev. B 36, 9219–9227.
Laufer, D., Pat-El, I., Bar-Nun, A., 2005. Experimental simulation of the formation of non-circular active depressions on Comet Wild-2 and of ice grain ejection from cometary surfaces. Icarus 178, 248–252.
Li, J.-Y., and 10 colleagues, 2007. Deep Impact photometry of Comet 9P/Tempel 1. Icarus 187, 41–55.
Paterson, W.S.B., 1994. The Physics of Glaciers. Butterworth Heinemann, Oxford.
Richardson, J.E., Melosh, H.J., Lisse, C.M., Carcich, B., 2007. A ballistics analysis of the Deep Impact ejecta plume: Determining Comet Tempel 1's gravity, mass, and density. Icarus 190, 357–390.
Sunshine, J.M., and 22 colleagues, 2006. Exposed water ice deposits on the surface of Comet 9P/Tempel 1. Science 311, 1453–1455.
Sunshine, J.M., Groussin, O., Schultz, P.H., A'Hearn, M.F., Feaga, L.M., Farnham, T.L., Klaasen, K.P., 2007. The distribution of water ice in the interior of Comet Tempel 1. Icarus 190, 284–294.
Thomas, P.C., and 14 colleagues, 2007. The shape, topography, and geology of Tempel 1 from Deep Impact observations. Icarus 187, 4–15.